Available online at www.sciencedirect.com
ScienceDirect
Trans. Nonferrous Met. Soc. China 20(2010) 1545−1549
Transactions of Nonferrous Metals Society of China
www.tnmsc.cn

Synthesis and electrochemical performance of $Li_3V_2(PO_4)_3$ by optimized sol-gel synthesis routine

ZHANG Qian(张 倩)[1], LI Yan-hong(李艳红)[2], ZHONG Sheng-kui(钟胜奎)[3], XIAO Xin-he(肖新和)[4], YAN Bo(颜 波)[3]

1. Department of Biological and Chemical Engineering, Guangxi University of Technology, Liuzhou 545006, China;
2. Guangxi Key Laboratory of Environmental Engineering, Protection and Assessment, College of Environmental Science and Engineering, Guilin University of Technology, Guilin 541004, China;
3. Department of Material and Chemical Engineering, Guilin University of Technology, Guilin 541004, China;
4. Hunan Institute of Humanities, Science and Technology, Loudi 417000, China

Received 6 July 2009; accepted 5 January 2010

Abstract: $Li_3V_2(PO_4)_3$ samples were synthesized by sol-gel route and high temperature solid-state reaction. The influence of $Li_3V_2(PO_4)_3$ as cathode materials for lithium-ion batteries on electrochemical performances was investigated. The structure of $Li_3V_2(PO_4)_3$ as cathode materials for lithium-ion batteries and morphology of $Li_3V_2(PO_4)_3$ were characterized by X-ray diffractometry (XRD) and scanning electron microscopy (SEM). Electrochemical performances were characterized by charge/discharge and AC impedance measurements. $Li_3V_2(PO_4)_3$ with smaller grain size shows better performances in terms of the discharge capacity and cycle stability. The improved electrochemical properties of $Li_3V_2(PO_4)_3$ are attributed to the refined grains and enhanced electrical conductivity. AC impedance measurements also show that the $Li_3V_2(PO_4)_3$ synthesized by sol-gel route exhibits significantly decreased charge-transfer resistance and shortened migration distance of lithium ions.
Key words: lithium ion batteries; cathode material; $Li_3V_2(PO_4)_3$; sol-gel method

1 Introduction

Since lithium iron phosphate was first reported as cathode material for lithium-ion batteries by PADHI et al[1] in 1997, the framework materials based on the phosphate polyanion have been identified as potential electroactive material for lithium and lithium ion battery applications. Some other transition phosphate polyanion insertion hosts such as $Li_3V_2(PO_4)_3$[1−3], $LiVPO_4F$ [4−10], $LiFePO_4$[11−14] and $LiMnPO_4$[15] are proposed as a new class of cathode materials for lithium-ion batteries because of their stable framework, relatively high voltage, good lithium ion transport and large theoretical capacity. With relatively high capacity and suitable operating voltage for the present commercial electrolyte system, $Li_3V_2(PO_4)_3$ is considered to be one of the most promising cathode materials among the above-mentioned phosphate polyanion hosts. Monoclinic $Li_3V_2(PO_4)_3$ forms a three-dimensional (3D) framework that contains three independent lithium sites.

In this work, $Li_3V_2(PO_4)_3$ samples were synthesized by two different routes, and the resulting electrochemical lithium extraction/insertion properties were investigated.

2 Experimental

2.1 Synthesis of $Li_3V_2(PO_4)_3$

The sol-gel route included two main processes. Firstly, $V_2O_5{\cdot}nH_2O$ hydro-gel was prepared. V_2O_5 was melted in a crucible by heating at 700 °C for 2 h; the molten V_2O_5 was poured into water; then a red brown solution was formed in a stainless steel container. Product was obtained by keeping the solution at room temperature for 10 h. Secondly, citric acid with equivalent amount-of-substance to V_2O_5 and stoichiometric amounts of $NH_4H_2PO_4$ and Li_2CO_3 were added into the above $V_2O_5{\cdot}nH_2O$ hydro-gels. The

Foundation Item: Projects(0991025, 0842003-5 and 0832259) supported by Natural Science Foundation of Guangxi Province, China; Project supported by the Joint Graduate Innovation Talent Cultivation Base of Guangxi Province, China; Project(GuiJiaoRen [2007]71) supported by the Research Funds of the Guangxi Key Laboratory of Environmental Engineering, Protection and Assessment Program to Sponsor Teams for Innovation in the Construction of Talent Highlands in Guangxi Institutions of Higher Learning, China
Corresponding author: ZHONG Sheng-kui; Tel: +86-773-5896446; Fax: +86-773-5896436; E-mail: zhongshk@glite.edu.cn
DOI: 10.1016/S1003-6326(09)60336-8

mixture was strongly stirred at room temperature for 2 h, and finally dried at 80 °C in an oven. The mixture was pressed into pellets and heated at 300 °C in a tubular furnace with flowing argon gas for 4 h to decompose and obtain the precursor. The precursor was then ground, pressed into pellets again, heated to 600 °C and held for 30 h in flowing argon gas to obtain the $Li_3V_2(PO_4)_3$ samples. The samples prepared through sol-gel route were abbreviated to $Li_3V_2(PO_4)_3$ (S).

For comparison, $Li_3V_2(PO_4)_3$ samples were also synthesized by high temperature solid-state reaction. The process was as follows. Stoichiometric $LiOH·H_2O$, V_2O_5, $NH_4H_2PO_4$ and 30 % (mass fraction) excess sucrose were used as starting materials. The mixture was initially heated to 300 °C in argon gas for 4 h to decompose and obtain the precursor. The precursor was then ground, pressed into pellets, heated to 900 °C and held for 30 h in flowing argon gas. The samples prepared through high temperature solid-state reaction were abbreviated to $Li_3V_2(PO_4)_3$ (H).

2.2 Physical characterization

X-ray diffractometer (XRD, Rint-2000, Rigaku) was employed to identify the crystalline phase of the synthesized materials. The particle size and morphology of the $Li_3V_2(PO_4)_3$ powders were observed with scanning electron microscope (JEOL, JSM-5600 LV) at an accelerating voltage of 15 kV. The content of carbon was determined by a carbon-sulfur analyser (Multi EA2000).

2.3 Electrochemical test

The $Li_3V_2(PO_4)_3$ electrodes were prepared by mixing acetylene black, polyvinylidene fluoride (PVDF), and 1-methl-2-pyrrolidone in acetone to ensure homogeneity. The mass ratio of active material, acetylene black and PVDF in the electrodes was 80: 10:10 except for special statement. The resulting slurry was pasted on an aluminium foil current collector with a diameter of 12 mm. After being dried at 120 °C in a vacuum oven for 24 h, the resulting electrodes with an active material load of about 8 mg/cm^2 were transferred to an Ar-filled glove box to assemble testing cells which included $Li_3V_2(PO_4)_3$ cathode, lithium metal anode and Celguard-2300 separator placed between the cathode and anode. The electrolyte was 1 mol/L $LiPF_6$ in a mixture of ethylene carbonate (EC) and dimethyl carbonate (DMC) with a volume ratio of 1:1. The cells were charged and discharged over a voltage range from 3.0 to 4.4 V versus Li/Li^+ electrode. Electrochemical impendence spectrum (EIS) measurements were performed covering a frequency range from 10 kHz to 10 mHz with an AC voltage of 5 mV. The EIS experiments were performed in the three-electrode system using lithium metal foil as both counter and reference electrode.

3 Results and discussion

Fig.1 shows the XRD patterns of $Li_3V_2(PO_4)_3$ (H) and $Li_3V_2(PO_4)_3$ (S). All fundamental peaks can be indexed to the monoclinic structure (space group $P2_1/n$) for both samples. These results are in good agreement with previous reports[1−4]. In addition, the XRD patterns of the two samples are similar, indicating that the different synthesis methods do not change the monoclinic structure.

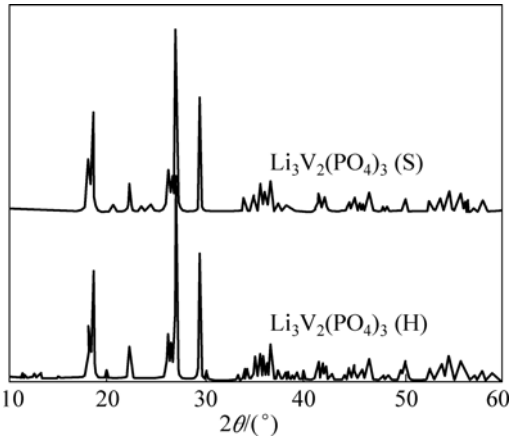

Fig.1 XRD patterns of $Li_3V_2(PO_4)_3$

SEM images of $Li_3V_2(PO_4)_3$ are shown in Fig. 2. It is obvious that the particle size of $Li_3V_2(PO_4)_3$ differs greatly, $Li_3V_2(PO_4)_3$ (H) consists of larger and non-uniform particles, while $Li_3V_2(PO_4)_3$ (S) has smaller particle size of about 0.6 μm. This indicates that the sol-gel route inhibits the particle growth during the sintering process. In addition, for both samples, the surface is rough, some small particles which bound on the surface of $Li_3V_2(PO_4)_3$ are observed, and they can be considered as small scattered carbon particles. This observation is consistent with the carbon-coated $LiCoO_2$ and $LiFePO_4$, in which sucrose was used as carbon source.

The first charge−discharge curves of $Li_3V_2(PO_4)_3$ samples between 3.0 and 4.4 V at a rate of 0.5*C* are shown in Fig.3. For both samples, the shapes of charge and discharge curves are similar. However, the initial charge and discharge capacities of $Li_3V_2(PO_4)_3$ (H) and (S) are different. The initial charge and discharge capacities of $Li_3V_2(PO_4)_3$ (H) are about 131 and 119 mA·h·g^{-1}, respectively, and the columbic efficiency of the initial charge−discharge cycle is about 90.84%. The initial charge and discharge capacities of $Li_3V_2(PO_4)_3$ (S) are about 136 and 128 mA·h·g^{-1}, respectively, and the columbic efficiency of the initial charge−discharge cycle is about 94.12%. Obviously, the initial charge and discharge performance of $Li_3V_2(PO_4)_3$ (H) was worse

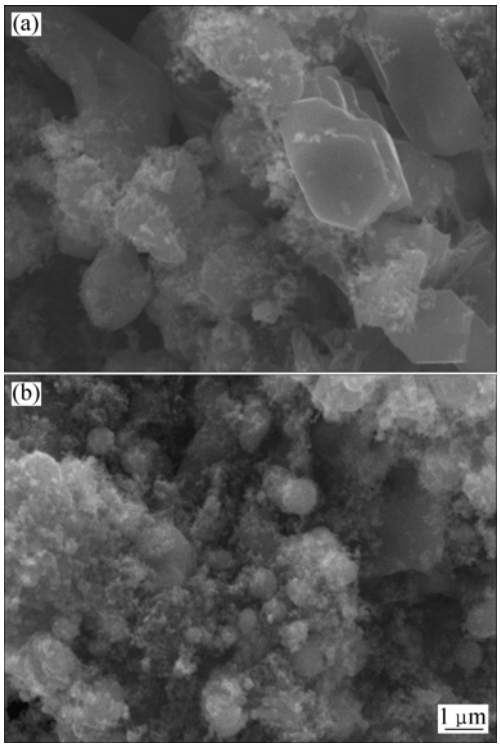

Fig.2 SEM images of samples $Li_3V_2(PO_4)_3$

than that of $Li_3V_2(PO_4)_3$ (S).

The electrochemical cycling performance of $Li_3V_2(PO_4)_3$ (H) and $Li_3V_2(PO_4)_3$ (S) was evaluated in the Li/$Li_3V_2(PO_4)_3$ cell configuration in a voltage range of 3.0−4.4 V at room temperature. Fig.4 shows the cyclic charge−discharge profiles of the $Li_3V_2(PO_4)_3$ cathode materials at different rates. As seen in Fig.4, after 50 cycles, the $Li_3V_2(PO_4)_3$ (H) sample exhibits a discharge capacity of about 100, 95 and 89 $mA{\cdot}h{\cdot}g^{-1}$ at the rates of 0.5*C*, 1.0*C* and 1.5*C*, respectively. Namely, after 50 cycles, the capacity loss is about 15.97% at 0.5*C*, 20.17% at 1.0*C* and 25.21% at 1.5*C*. Whereas, after 50 cycles, the $Li_3V_2(PO_4)_3$ (S) sample exhibits a discharge capacity about 117, 110 and 107 $mA{\cdot}h{\cdot}g^{-1}$ at the rates of 0.5*C*, 1.0*C* and 1.5*C*, respectively. Namely, after 50 cycles, the capacity loss is about 8.59% at 0.5*C*, 14.06% at 1.0*C* and 16.41% at 1.5*C*. From the above results, it can be concluded that $Li_3V_2(PO_4)_3$ sample synthesized by the sol-gel route has better cycling performance than that synthesized by high temperature solid-state reaction. The excellent electrochemical-cycling stability of the electrode can be attributed to the decrease of grain size and improved homogeneity of the carbon dispersion.

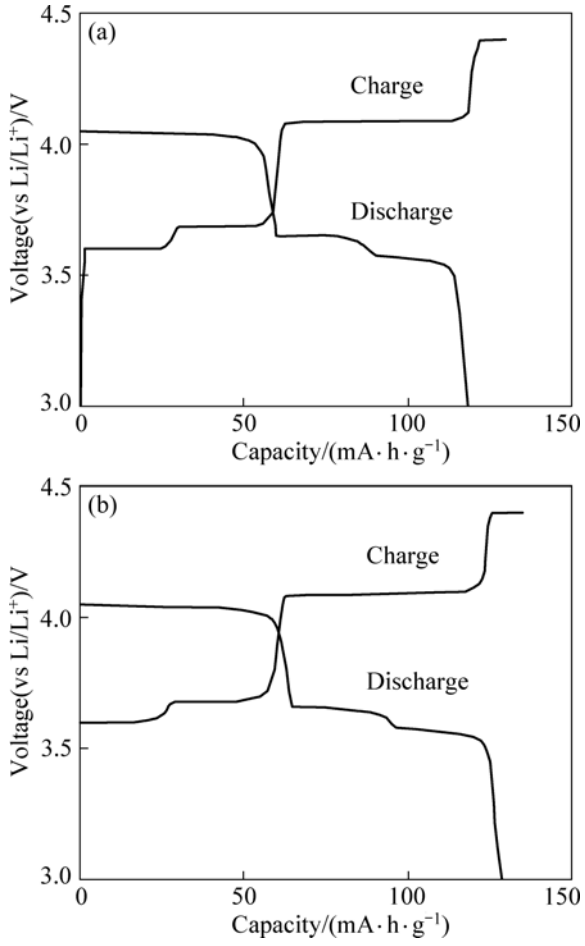

Fig.3 First charge-discharge curves of $Li_3V_2(PO_4)_3$ (H) (a) and $Li_3V_2(PO_4)_3$ (S) (b)

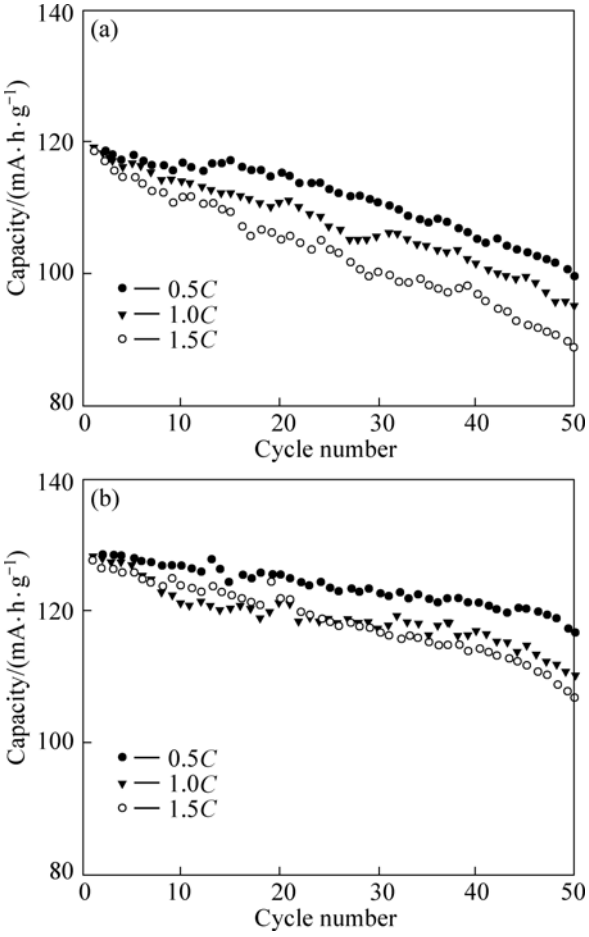

Fig.4 Electrochemical cycling performance of $Li_3V_2(PO_4)_3$ (H) (a) and $Li_3V_2(PO_4)_3$ (S) (b)

The electrochemical impedance spectra (EIS) of $Li_3V_2(PO_4)_3$ (H) and (S) electrode materials were measured at different charging states. The typical Nyquist plots for EIS of both samples are presented in Fig.5. Similar EIS patterns are observed for both samples. A semi-circle is observed at the high frequency range. In the low frequency range, a straight line of 45° to the real axis corresponds to the Warburg impedance. The high frequency semi-circle is related to the charge-transfer resistance (R_{ct}) and the double-layer capacitance, and the low frequency tails result from the diffusion of lithium ions in the bulk active mass. In the case of $Li_3V_2(PO_4)_3$ (S), the diameter of the semi-circle significantly depends on the potential during charging, indicating that the film formation process is dependent on the lithium ion content. On the other hand, R_{ct} shows a greater dependence on the lithium insertion and extraction levels. In the highly charged states, the sample was found to exhibit lower R_{ct}. By comparing the diameter of the semi-circle in the two systems, it can be found that $Li_3V_2(PO_4)_3$ (S) shows lower R_{ct} value than $Li_3V_2(PO_4)_3$ (H), indicating that sol-gel route may increase the electronic conductivity and improve the Li^+ kinetic behavior.

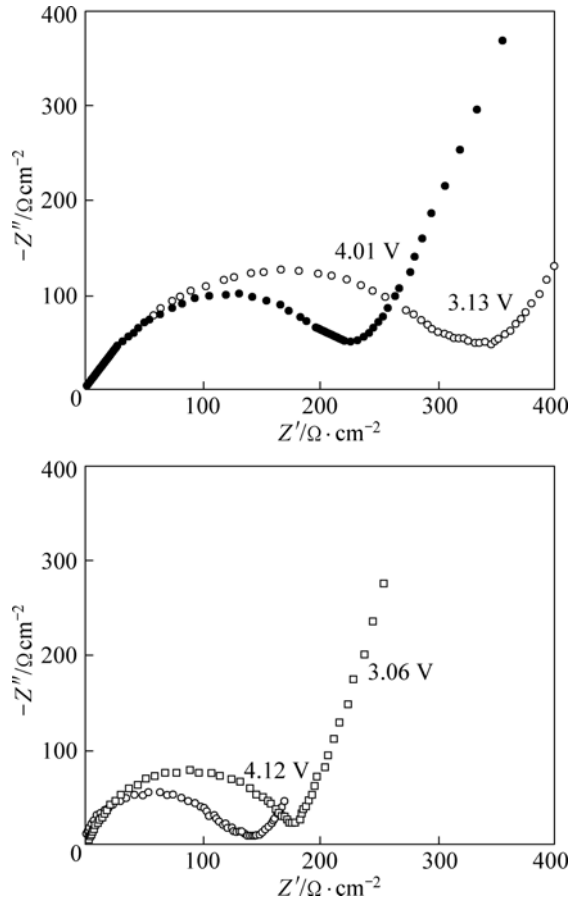

Fig. 5 Nyquist plots for EIS of $Li_3V_2(PO_4)_3$ at different charge states

The electronic conductivities of $Li_3V_2(PO_4)_3$ (H) and (S) samples are 6.5×10^{-8} and 1.4×10^{-6} S/cm, respectively, measured with the four-electrode. The conductivity of $Li_3V_2(PO_4)_3$ (S) is about a factor of 10^2 higher than that of $Li_3V_2(PO_4)_3$ (H). Lithium insertion and extraction in $Li_3V_2(PO_4)_3$ electrodes are accompanied by electron transfer on the particle surface. In sol-gel route, low synthesized temperature inhibits the growth of particle during sintering, which enhances the electronic conductivity of the electrode materials, so electron transfer in $Li_3V_2(PO_4)_3$ (S) would be more facilitated than that in $Li_3V_2(PO_4)_3$ (H). As a result, the $Li_3V_2(PO_4)_3$ prepared by sol-gel route demonstrates better electrochemical performance at high rate.

4 Conclusions

1) Two synthesis routes were investigated and the electrochemical properties of the $Li_3V_2(PO_4)_3$ samples were compared. The grain size of $Li_3V_2(PO_4)_3$ sample is significantly smaller than that of the sample synthesized through sol-gel route.

2) The $Li_3V_2(PO_4)_3$ (S) sample exhibits a much higher discharge capacity and lower capacity loss than $Li_3V_2(PO_4)_3$ (H) after 50 cycles. It is confirmed that the sample prepared by sol-gel route decreases the resistances of the lithium-ion migration and charge transfer from electrochemical impedance measurements.

3) The improved electrochemical properties of the $Li_3V_2(PO_4)_3$ (S) are attributed to the decreased grain size and enhanced electrical conductivity. Sol-gel route proposed in this investigation may increase the possibility of the application $Li_3V_2(PO_4)_3$ to commercial lithium-ion batteries.

References

[1] PADHI A K, NANJUNDASWAMY K S, GOODENOUGH J B. Phospho-olivines as positive-electrode materials for rechargeable lithium batteries[J]. J Electrochem Soc, 1997, 144(4): 1188−1194.

[2] ZHONG S K, YIN Z L, WANG Z X, CHEN Q Y. Cathode material $Li_3V_2(PO_4)_3$: Low temperature solid-state reaction synthesis and performance [J]. Inorg Chem, 2006, 22: 1843−1846.

[3] LI Y Z, LIU X, YAN J. Study on synthesis routes and their influences on chemical and electrochemic performances of $Li_3V_2(PO_4)_3$/carbon [J]. Electrochim Acta, 2007, 52: 473−479.

[4] BARKER J, SAIDI M Y, SWOYER J L. Lithium metal fluorophosphates materials and preparation thereof. US 6387568B1 [P]. 2002-05-14.

[5] ZHONG S K, YIN Z L, WANG Z X, CHEN Q Y. Synthesis and characterization of the triclinic structural $LiVPO_4F$ as possible 4.2V cathode materials for lithium batteries [J]. J Cent South Univ Techno, 2007, 14(3): 340−343.

[6] LI Y Z, ZHOU Z, GAO X P, YAN J. A novel sol-gel method to synthesize nanocrystalline $LiVPO_4F$ and its electrochemical Li intercalation performances [J]. J Power Sources, 2006, 160: 633−637.

[7] BARKER J, SAIDI M Y, SWOYER J L. Electrochemical insertion properties of the novel lithium vanadium fluorophosphates, $LiVPO_4F$ [J]. J Electrochem Soc A, 2003, 150: 1394−1398.

[8] BARKER J, SAIDI M Y, SWOYER J. A comparative investigate of the Li insertion properties of the novel fluorophosphates phases, $NaVPO_4F$ and $LiVPO_4F$ [J]. J Electrochem Soc A, 2004, 151: 1670−1677.

[9] BARKER J, SAIDI M Y, GOVER R K B, BURNS P, BRYAN A. The effect of Al substitution on the lithium insertion properties of lithium vanadium fluorophosphate, $LiVPO_4F$ [J]. J Power Sources, 2007, 174: 927−931.

[10] BARKER J, GOVER R K B, BURNS P, BRYAN A, SAIDI M Y, SWOYER J L. Structural and electrochemical properties of lithium vanadium fluorophosphates, $LiVPO_4F$ [J]. J Electrochem Soc A, 2005, 152: 1776−1779.

[11] CHEN J M, HSU C H, LI Y R, HSIAO M H. High-power $LiFePO_4$ cathode materials with a continuous nano carbon network for lithium-ion batteries [J]. J Power Sources, 2008, 184: 498−502.

[12] JIN B, JIN E M, HEE K P, GU H B. Electrochemical properties of $LiFePO_4$–Multiwalled carbon nanotubes composite cathode materials for lithium polymer battery [J]. Electrochem Commun, 2008, 10: 1537−1540.

[13] HIROSE K, HONMA T, DOI Y, HINATSU Y, KOMATSU T. Mössbauer analysis of Fe ion state in lithium iron phosphate glasses and their glass-ceramics with olivine-type $LiFePO_4$ crystals [J], Solid State Commun, 2008, 146: 273−277.

[14] MI C H, ZHANG X G, ZHAO X B, LI H L. Effect of sintering time on the physical and electrochemical properties of $LiFePO_4$/C composite cathodes [J]. J Alloys Compd, 2006, 424: 327−333.

[15] FANG H S, LI L P, LI G S. Hydrothermal synthesis of electrochemically active $LiMnPO_4$ [J]. Chem Lett, 2007, 36: 436−437.

(Edited by FANG Jing-hua)